Use of Digital Image Correlation for Validation of Surface Strain in Specimen-specific Vertebral Finite Element Models

H. M. Gustafson[1,2] and P. A. Cripton[1,2]
[1] Orthopaedics and Injury Biomechanics Laboratory, University of British Columbia;
[2] International Collaboration on Repair Discoveries, Vancouver, BC Canada

ABSTRACT

Finite element (FE) models of the spine are typically validated to be similar to the average experimental response of specimens with anatomical variation, such as varying sizes and degrees of degeneration. To account for this variation in a manner that allows validation against a specific vertebral response instead of an average range, specimen-specific models can be developed. The purpose of this study was to compare the strain predicted by specimen-specific FE models of vertebrae under compressive loading with the strain measured experimentally using digital image correlation (DIC), a non-contact optical method. A secondary purpose was to compare the DIC measured strain with strain gauges to verify the use of DIC for obtaining full field strain. DIC has not been used to investigate cadaveric vertebrae previously. Fresh-frozen human cadaveric vertebrae (n = 6) from three donors were obtained. A high resolution CT scan of each bone was taken and the bone was segmented from the CT images to create geometric models for the FE analysis. For the experiment, the vertebrae were tested in a materials testing machine. The bone was loaded dynamically to failure at a rate of 0.5 m/s. For the FE model, heterogeneous Young's modulii were assigned to each of the trabecular elements. A displacement function was applied at the superior endplate based on the experimental measurements. Before the loading, the average error between the DIC measured strain and strain gauge was 105.2 microstrain while during the loading it was 417.3 microstrain. We judged this error in the DIC acceptable to use for model validation. The minimum principal strains from the experiment and FE model were compared qualitatively and quantitatively. The coefficients of determination for the quantitative comparisons were between 0.15 and 0.41. The similarity shows the potential of the specimen-specific models to predict surface strain, but further refinement of the models is needed. Use of DIC provides a unique and detailed dataset for validation of specimen-specific models.

INTRODUCTION

In the United States, it is estimated that there are approximately 12,000 new spinal cord injuries (SCIs) each year and 273,000 people living with a SCI (NSCISC, 2013). In Canada there are approximately 4,300 new SCIs each year, and today more than 86,000 people are living with a SCI (Farry, 2010). Injuries to the spinal cord are strongly associated with the incidence of vertebra fracture. In a retrospective study of spinal cord injuries treated at a Canadian care center over a four year period, fracture was associated with 56% (63/113) of cases of injury to the cervical spinal cord and 100% (27/27) of cases of injury to the thoracic spinal cord (Pickett, 2006). In a review of 562 cases of traumatic vertebra fracture in Germany, it was reported that the average age of the patients was 43.8 years showing the relatively young age at which patients sustain these injuries (Leucht, 2009). Furthermore, it was also observed that the majority of the patients sustained compression fractures (54.8%) as compared to fractures due to distraction or rotation (Leucht, 2009). These findings highlight the need to understand spinal compression fractures to help reduce the incidence of fractures and avoid the serious consequences of SCIs.

Spine injuries can be studied in the laboratory setting, but it can be difficult to relate experimental findings to the clinical population since unlike many patients who sustain vertebrae fractures, cadaveric donors tend to be elderly and may have degenerated spines. The age and degeneration can also lead to disparate results in the same test making it difficult to determine an average response. One way to overcome these limitations is through the use of specimen-specific finite element (FE) models. Specimen-specific models match the specimen's bone geometry and incorporate varying material properties based on the particular specimen's bone density. If simulation results match those from an experiment, the models can be modified to predict how a bone might fracture in a younger population when there is non-degenerated bone geometry and higher bone density.

One measure that can be compared between experiments and FE models is the surface strain. Strain can be measured using strain gauges; however, strain gauges only capture a small area and the area may not be the location of highest strain. An alternative approach is use of digital image correlation (DIC). DIC is a non-contact optical measurement technique that can be used to calculate the full-field deformation and strain on a surface (Pan, 2009). If more than one camera is used to image a surface, three-dimensional deformations and strains can be calculated. To perform the correlation calculations, DIC requires the surface to have a varying intensity pattern. The pattern may be applied to the object or may be native to the object. For the DIC analysis, a subset of pixels in the undeformed state is identified. The same subset of pixels can then be identified in the deformed states by identifying the location of maximum normalized cross correlation. This provides full-field strain data that can be used for validation.

Specimen-specific models have been used to successfully predict fracture risk under quasi-static compressive loading of thoraco-lumbar vertebrae (Crawford, 2003; Imai, 2006; Liebschner, 2003; Silva, 1998). However, few have been validated using experimentally measured strain and none have used the full-field information available with DIC. Furthermore, to our knowledge, specimen-specific FE models have not been used to investigate dynamic loading or upper thoracic and cervical vertebral fracture. The goals of this work were to

2

compare the strain predicted by specimen-specific FE models of vertebrae under compressive loading with the strain measured experimentally using DIC and to judge if the specimen-specific FE analysis approach merits further investigation. Additionally, a secondary goal was to compare the DIC measured strain with strain gauges to verify the DIC measurements.

METHODS

Experimental

For this work, cervical and thoracic vertebrae (n = 6) were obtained from three cadaveric donors; the average age of specimens was 70.1 (SD ±3.2) years. The levels of the vertebrae were C6, T1 (n = 3), T2, and T3. The bones were scanned in a high-resolution peripheral quantitative computed tomography (HR-pQCT) scanner (Xtreme CT, Scanco, Switzerland) with an isotropic resolution of 246 μm. During preparation and testing, the bones were kept hydrated with saline.

The bones were cleaned, and all soft tissue was removed, including the periosteum. Polymethylmethacrylate (PMMA) was molded to the superior and inferior surfaces of the bone. The bone was aligned so that the anterior and posterior midline points on the superior endplate were parallel to the ground and the superior endplate was aligned symmetrically about the midline.

A small area of the bone near the inferior edge of the anterior body was prepared for a strain gauge. The area was scraped using a scalpel blade and cleaned with Acetone and 2-propanol. A triaxial strain rosette (model FRA-1-11-3LT, TML, Japan) was then applied. Following gauge application, a small drop of cyanoacrylate was used to secure the PMMA to the vertebrae, and the strain gauge wires were glued to the PMMA for strain relief. The bones were then painted with a thin layer of white paint, and then an airbrush was used to apply a black speckle pattern to the bone for tracking using DIC (Figure 1).
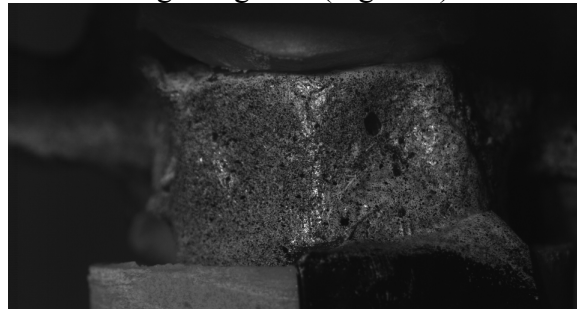

Figure 1: Example of a prepared T1 specimen with the speckle pattern applied on the vertebra.

For the testing, the vertebrae were loaded in a materials testing machine (8874, Instron Corporation, USA). The bones were initially preloaded to approximately 30 N. Coordinates of points on the bone and the experimental setup were digitized (Optotrak Certus, Northern Digital Inc., Canada). The bone was imaged using two high-speed cameras (Phantom V12s, Vision Research, USA) that captured the anterior surface of the bone. The vertebrae were first loaded quasi-statically in compression to 800 N over 5 s, and images were captured at 100 Hz. Next, the vertebrae were loaded to failure at 0.5 m/s, and images were captured at 10,000 Hz.

3

Accuracy Investigation

To explore the accuracy of DIC, a square rod of a thermoplastic material, Delrin, was potted in PMMA. The rod preparations were similar to previous methods for the vertebrae. The surface of the material was prepared, and a strain rosette was applied. A thin layer of white paint was pained over the strain gauge and the surface of the sample. Then, an airbrush was used to apply a black speckled pattern. The sample was preloaded to 30 N and then compressed in the materials testing machine at a rate of 600 N/s for 5 seconds. The strains were extracted over the area of the strain gauge using DIC software (StrainMaster, LaVision Inc., Germany).

Computational Model

For the computational model, six specimen-specific models were developed. First, the vertebrae were semi-automatically segmented from the HR-pQCT images (AnalyzeDirect Inc. USA). The bone geometry was then manually repaired to create geometry that could be meshed (Rapidform, INUS Technology, South Korea). The cortical shell geometry was created by offsetting the bone surface by 0.4 mm inwards. The cortical shell and trabecular core were meshed with second-order tetrahedral elements with edge lengths of approximately 1 mm (Hypermesh, Altair Engineering Inc., USA). To account for variation in the bone density, heterogeneous materials properties were assigned using open-source software (Bonemat V3, B3C, Italy) based on the relationship established for lumbar vertebrae (Morgan, 2003).

$$E = 4.730\rho_{app}^{1.56}$$

where E is the Young's modulus of the element and ρ_{app} is the apparent density of the bone.

The heterogeneous trabecular core and the homogeneous cortical bone were imported into an explicit FE solver (Pam-Crash, ESI Group, France). The cortical shell was assigned constant linear elastic material properties (E = 16.8 and ν = 0.3). The inferior nodes of the vertebral body were constrained to be stationary. A displacement boundary obtained from the high-speed cameras was applied to the superior nodes of the vertebral body in a local coordinate frame that matched the experimental loading. Failure was not modeled. The minimum principal strain was computed.

Data Processing

The images from the experiments up to the point where initial failure was observed on the surface of the bone were processed using the DIC software. The region size for analysis was 31 x 31 pixels with overlap of 16 pixels and analysis was performed relative to the undeformed image. In the DIC software, the area over the strain gauge was identified, and the minimum principal strain was exported. For comparison with the computational model, the minimum principal strain was exported as a two-dimensional map. The computational results were manually aligned to the DIC orientation and corresponding rectangular regions were selected for analysis. Average values of the minimum principal strains were calculated for squares of pixels in the experimental and computational results. These results were plotted against each other and the coefficient of determination (R^2) was found. The 95% confidence intervals were determined for the regression lines.

4

RESULTS

For the Delrin thermoplastic sample, the correspondence of the minimum principal strains between the strain gauges and the DIC was strong (Figure 2). The DIC signal was noisier than the strain gauge signal, but the shape and locations of the peaks matched well. The average difference in the strains was 104 microstrain with only the preload applied and 216 microstrain during loading.
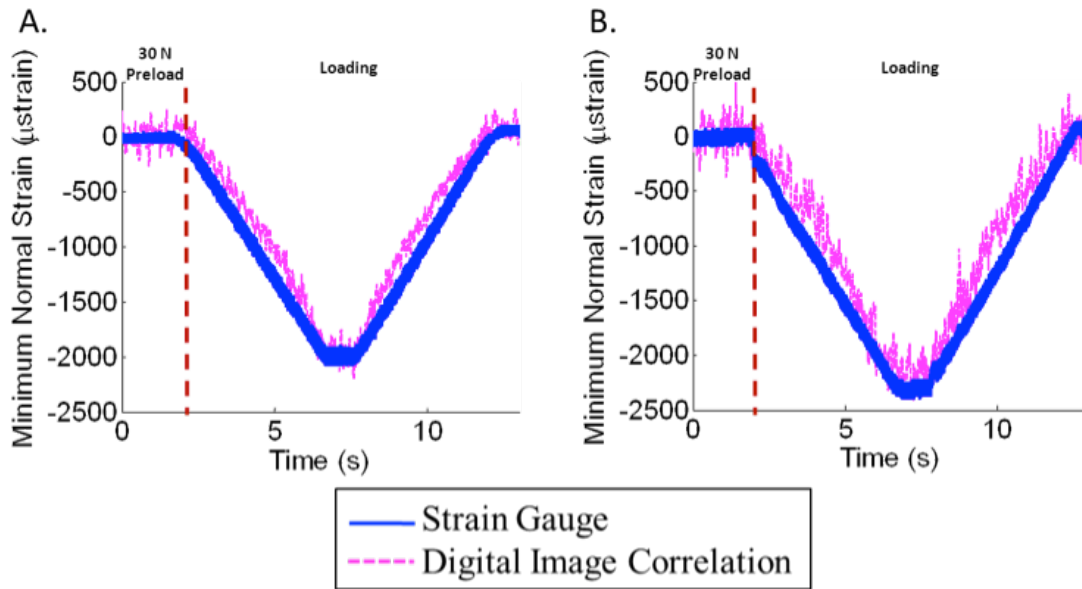

Figure 2: Comparison of the minimum principal strains as measured by the strain gauge and the DIC in two different tests with a Delrin sample.

For the vertebrae, the minimum principal strain from the strain gauges and the DIC analysis had similar shapes (Figure 3). The average difference between the strains was 105.2 microstrain with only the preload applied and 417.3 microstrain during loading (Table 1). For Donor 3 T3 the strain gauge failed so the comparison is not provided.
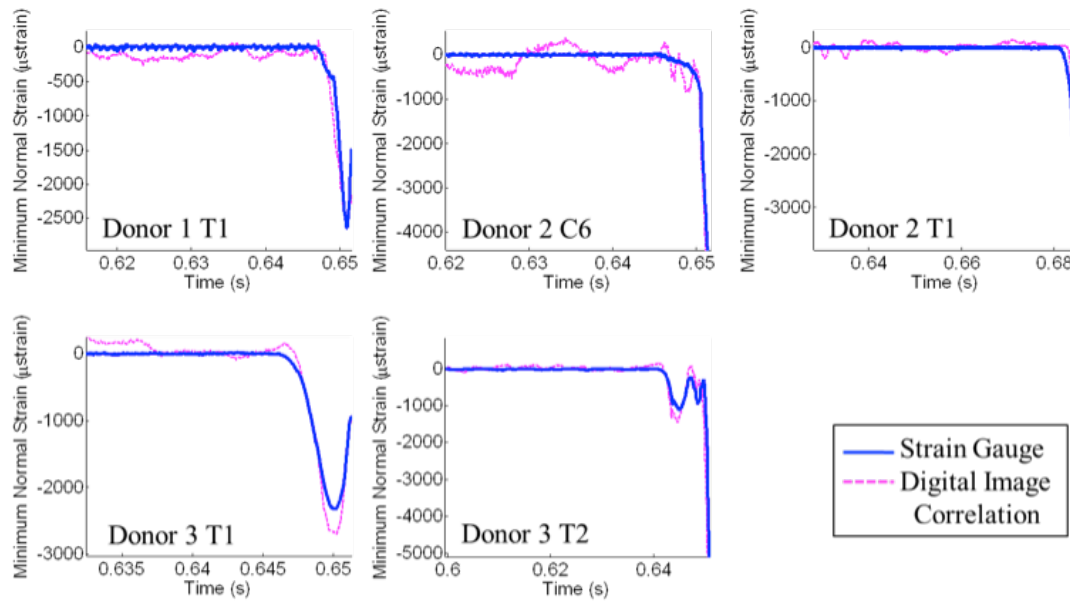
5

Figure 3: Minimum principal strain on the surface of the vertebrae measured using tri-axial strain gauges (blue, solid) and DIC at the locations of the strain gauges (magenta, dashed).

Table 1: Average difference between the strain gauge and the DIC strain before the loading and as the loading is occurring

	Error with only the preload applied (microstrain)	Loaded error (microstrain)
Donor 1, T1	85.0	288.7
Donor 2, C6	237.5	828.3
Donor 2, T1	59.5	280.3
Donor 3, T1	91.5	180.7
Donor 3, T2	52.6	509.7
Average	**105.2**	**417.3**

A qualitative comparison of the results shows that the areas of high compressive strain are observed in both the FE models and the experiments (Figure 4). Quantitatively, the coefficients of determination (R^2) ranged from 0.15 to 0.41 for the minimum principal strain from the computational models versus from the DIC analysis (Figure 5). For the regression lines, the slopes ranged from 0.18 to 1.15 and the y-axis intercepts ranged from -879 to -7577 microstrain (Table 2).
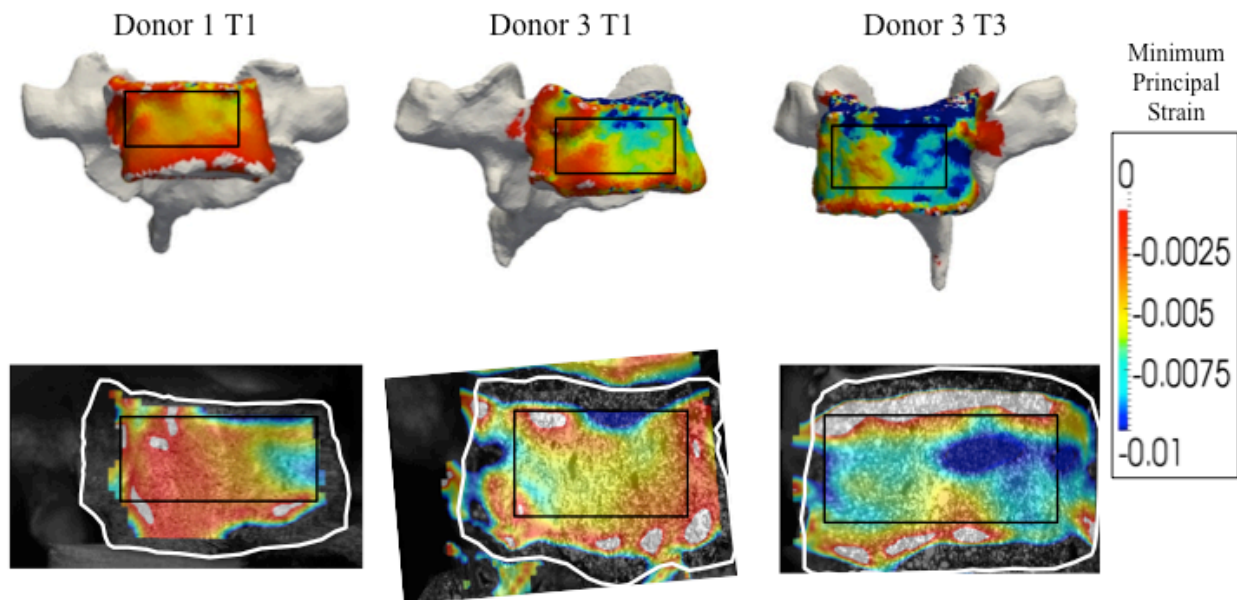
6

Figure 4: Qualitative comparison between the specimen-specific FE models (top) and the experimental DIC results (bottom) prior to failure on the anterior surface. The white outlines indicate the location of the bone in the high-speed images. The black boxes indicate the approximate region over which the comparison was made between the models and the experiments.
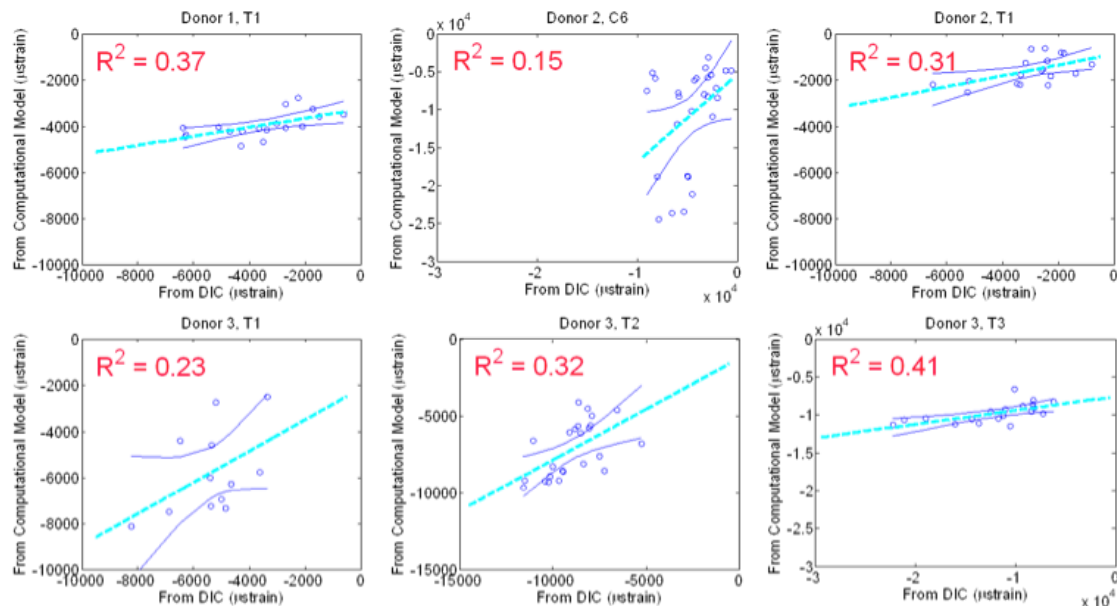

Figure 5: Quantitative comparison between the computational model and the DIC results. The regression lines (cyan, dashed) and the confidence intervals for the regression lines (blue, solid) are provided.

Table 2: Summary of the slopes and the y-axis intercepts of the regression lines for the FE predicted strain vs. the DIC measured strain

	Slope	Intercept (microstrain)
Donor 1, T1	0.20	-3270
Donor 2, C6	1.15	-5353
Donor 2, T1	0.24	-879
Donor 3, T1	0.68	-2148
Donor 3, T2	0.66	-1281
Donor 3, T3	0.18	-7577

DISCUSSION

The goals of this work were to determine how well specimen-specific FE models could predict the experimental strains in a compressive test with cadaveric cervical and upper thoracic vertebrae and if this approach merits further development in future. By creating specimen-specific models, it is hoped that the models can be used to predict fracture with FE models more representative of the clinical population that sustains vertebral fractures. Additionally, this work investigated the accuracy of DIC on a flat polymeric surface and on more complex human cadaveric vertebrae. The DIC strains were compared to the strains measured with a strain gauge, a transducer considered a gold standard in the present work.

For the comparison of the DIC and the strain gauge on the Delrin, the DIC generally measured lower compressive strains than the strain gauge, particularly during the loading and unloading. It is not clear if this bias is due to the strain gauge or the DIC. However, the goal was to determine if the accuracy was acceptable and an error of less than 10% of the strain at maximum load was deemed reasonable. For the DIC and the strain gauge on the vertebrae, the error was similarly accurate.

In the qualitative comparison between the FE models and the DIC, similarity can be seen, in particular with the areas of high compressive strain. For the quantitative comparison, the R^2 values were positive indicating that the strain pattern is capturing the same trend observed in the models, but the low values for R^2 also indicate that the models are not fully predicting the strain pattern. Furthermore, if the strain magnitudes from the model were matching the experiments, the slopes of all the regression lines would be 1. Our results, with slopes varying from 0.18 to 1.15, indicate that the current method of modeling is not predicting the magnitudes of the strain well and that refinement of the models is needed.

Previous experiments have used thoraco-lumbar vertebrae FE models to predict the stiffness, failure load, yield load, and strain (Liebschner, 2003; Crawford, 2003; Silva, 1998; Imai, 2006). When comparing the model predictions to the experimental results, R^2 values between 0.79 and 0.96 have been found for the stiffness and load values. Only one study to our knowledge has compared the strain between a vertebral compression experiment and FE model (Imai, 2006). The correlation of determination for the strain gauge-measured strain to the FE-

8

predicted strain in that experiment was 0.70. This indicates that predicting strain at a particular location may be more difficult than predicting a global value for the vertebra such as stiffness or load. The study by Imai implemented a more complex FE model than is being used in our study.

The approach of using DIC for validation of specimen-specific models has been applied in composite long bones (Dickinson, 2011) and the pelvis (Ghosh, 2012). In both cases, the bones were loaded quasi-statically with linearly increasing loads. The R^2 values for the experimental and predicted strains were found to be 0.92 and 0.91 for the two studies, respectively. In these cases, the bony geometries were less curved and larger than vertebrae. This may allow for the DIC values to be more accurately measured as curved surfaces are known to decrease the accuracy of the DIC at the extremes of the curvature. Additionally, since the boundary conditions applied to the FE models were linear in these studies, a strong linear relationship would be expected in the strains. In the current study, the load was applied dynamically and each FE model was only compared at one point in time to the experiment.

There are both computational and experimental limitations in this work. For the experimental work, the compression was applied to the vertebrae through PMMA molded to the endplates. However, the homogeneous PMMA may not apply loading in the same way that an intervertebral disc, composed of annulus and nucleus regions, would *in vivo*. To perform DIC analysis, the anterior surface of the bone was painted. Efforts were made to apply only a thin layer of paint, but the paint may have affected the bone strain. Computationally, it was assumed that the cortical shell thickness was a constant magnitude of 0.4 mm. This value was based on literature where the minimum average value of the cortical shell in the cervical spine was found to be 0.41 mm (Panjabi, 2001). The smallest value was selected as the constant thickness, but the use of heterogeneous bone material properties likely resulted in higher stiffnesses at the cortical-trabecular interface, effectively resulting in a thicker cortical shell. The Young's Modulus-density relationship was established using trabecular samples taken from lumbar vertebrae but this relationship is being applied to cervical and thoracic spine modeling. Since the anatomies of vertebrae are similar between these regions, we think this is a reasonable approach. The boundary input for the vertebrae was displacement, which was assigned uniformly to the superior endplate. In the actual experiment, the displacements at all locations on the superior endplate may not have been the same, although no behaviour was observed in the high-speed video to suggest highly variable deformations at neighbouring sections of the superior endplate. Strain was only measured up to the point where failure was observed on the anterior surface of the bone. After this point, the strains cannot be reliably measured since the cortical shell is fractured and is no longer deforming. Finally, for the DIC and model comparisons, manual manipulation was used to align the FE model with the DIC strains. In the future, a three-dimensional computational registration will be used for alignment.

CONCLUSIONS

In summary, this work presents a method for validating the strain on the surface of specimen-specific FE vertebra models by obtaining experimental full-field strain data. The models predicted the strain patterns on the anterior surface of the vertebrae and thus we are encouraged to develop this technique further. With model refinement, it is expected that the FE-DIC strain

pattern correlation will be higher and the FE magnitudes will be more similar to the experiments. The bone model will eventually be used to predict fracture risk in young populations most likely to sustain traumatic vertebrae fractures.

ACKNOWLEDGEMENTS

REFERENCES

CRAWFORD, R.P., CANN, C.E., KEAVENY, T.M. (2003). Finite Element Models Predict In Vitro Vertebral Body Compressive Strength Better than Quantitative Computed Tomography. Bone 33(4), 744-750.

DICKINSON, A. S., TAYLOR, A. C., OZTURK, H., BROWNE, M. (2011). Experimental Validation of a Finite Element Model of the Proximal Femur using Digital Image Correlation and a Composite Bone Model. Journal of Biomechanical Engineering 133(1).

FARRY, A., BAXTER, D. (2010). The Incidence and Prevalence of Spinal Cord Injury in Canada. Rick Hansen Institute.

GHOSH, R., GUPTA, S., DICKINSON, A., BROWNE, M. (2012). Experimental Validation of Finite Element Models of Intact and Implanted Composite Hemi-pelvises Using Digital Image Correlation. Journal of Biomechanical Engineering 134(8).

IMAI, K., OHNISHI, I., BESSHO, M., NAKAMURA, K. (2006). Nonlinear Finite Element Model Predicts Vertebral Bone Strength and Fracture Site. Spine 31(16), 1789-1794.

LEUCHT, P., FISCHER, K., MUHR, G., MUELLER, E.J. (2009). Epidemiology of Traumatic Spine Fractures. Injury 40(2), 166-172.

LIEBSCHNER, M.A.K., KOPPERDAHL, D.L., ROSENBERG, W.S., KEAVENY, T.M. (2003). Finite Element Modeling of the Human Thoracolumbar Spine. Spine 28(6), 559-565.

MORGAN, E.F., BAYRAKTAR, H.H., KEAVENY, T.M. (2003). Trabecular Bone Modulus–density Relationships Depend on Anatomic Site. Journal of Biomechanics 36(7), 897-904.

NATIONAL SPINAL CORD INJURY STATISTICAL CENTER (2008). Spinal Cord Injury Facts and Figures at a Glance. National Spinal Cord Injury Statistical Center, Birmingham, AL.

PAN, B., QIAN, K., XIE, H., ASUNDI, A. (2009). Two-dimensional Digital Image Correlation for In-plane Displacement and Strain Measurement: a Review. Measurement Science and Technology 20(6), 1-17.

PANJABI, M.M., CHEN, N.C., SHIN, E.K., WANG, J.L. (2001). The Cortical Shell Architecture of Human Cervical Vertebral Bodies. Spine 26(22), 2478-2484.

PICKETT, G.E., CAMPOS-BENITEZ, M., KELLER, J.L., DUGGAL, N. (2006). Epidemiology of Traumatic Spinal Cord Injury in Canada. Spine 31(7), 799-805.

SILVA, M.J., KEAVENY, T.M., HAYES, W.C. (1998). Computed Tomography−based Finite Element Analysis Predicts Failure Loads and Fracture Patterns for Vertebral Sections. Journal of Orthopaedic Research. 16(3), 300-308.